MATERIALS CHEMISTRY FRONTIERS

CCS 中国化学会 CHINESE CHEMICAL SOCIETY

ICCAS

ROYAL SOCIETY OF CHEMISTRY

Hierarchical Metal-Organic Frameworks constrcuted from intergrowth for light hydrocarbons adsorption

Journal:	*Materials Chemistry Frontiers*
Manuscript ID	QM-RES-05-2020-000352.R1
Article Type:	Research Article
Date Submitted by the Author:	06-Aug-2020
Complete List of Authors:	Yin, Xinyang; Pennsylvania State University, Department of Chemical Engineering Zhang, Xueyi; Pennsylvania State University, Department of Chemical Engineering

Article

Hierarchical Metal-Organic Frameworks constrcuted from intergrowth for light hydrocarbons adsorption

Received 00th January 20xx,
Accepted 00th January 20xx

DOI: 10.1039/x0xx00000x

Xinyang Yin and Xueyi Zhang *

Hierarchical Metal Organic Frameworks (MOFs) are a type of MOF material with both micropores and mesopores. In this work, we demonstrate heterometallic hierarchical MOF particles formed by intergrowth of pillared MOFs. Pillared MOF $M^{I}_{2}(ndc)_{2}(dabco)$ (M^{I}=Co, Ni, Cu, Zn, ndc=naphthelenedicarboxylic acid, dabco=1,4-diazabicyclo[2.2.2]octane) particles were synthesized with various morphologies, on which $M^{II}_{2}(ndc)_{2}(dabco)$ (M^{II}=Co, Ni, Cu, Zn) particles were intergrown. The intergrown particles preserved the structure, crystallinity, and morphology of their respective primary particles, while creating additional mesoporosity for gas adsorption. Adsorption of hydrocarbons (CH_4, ethane, ethene, propane, and propene) at pressures up to 10 bar (absolute) was performed on the MOFs. The hierarchical MOFs have shown increased adsorption of hydrocarbons at low pressures, and IAST selectivity of propane/methane as high as 53 were observed (total pressure 1 bar, CH_4 mole fraction: 0.8), suggesting the hierarchical materials can be used for adsorptive removal of natural gas liquids from crude natural gas.

Metal-organic frameworks (MOFs) are three-dimensionally ordered porous materials consisting of metal nodes and organic linkers. The tunable chemistry of MOF materials gives them opportunities in applications involving molecular recognition, such as gas separation,[1-8] gas storage,[9,10] catalysis,[11] and sensing.[12,13] The combination of two or more MOF structures in one crystal can further broaden their applications, where the precision of molecular recognition can be optimized. For example, Deng et al. introduced the multivariate MOFs (MTV-MOFs) for adsorptive CO_2/CO separation, in which multiple linkers are included in one unit cell with tunable linker distribution within one particle.[14] Functionalization of MOFs pioneered by Cohen et al. is another straightforward method to modify existing MOFs to include additional features.[15] In addition to modifying the linkers, post-synthesis exchange of linkers and ions brings two or more features into one MOF framework.[16] Above the molecular level, intergrowth of two or more MOF crystals combines their chemistry in one particle at the nanoscale and microscale. Intergrown MOF particles with various configurations, such as core-shell (isotropic)[17-20] and intergrowth on specific crystal facets (anisotropic), have also been prepared.[19-22] However, the above studies have shown that although additional features can be prepared in one MOF particle by intergrowth, the gas adsorption capacity and selectivity were not significantly increased becauase the MOF pore sizes are unchanged in those studies. It is therefore conceivable that introducing larger pores is one way to increase gas adsorption amount beyond this limit, with the additional opportunity of capturing and recognizing larger molecules. Recitular synthesis is a systematic way to control and extend MOF pore size.[23-25] However, the synthesis of their linkers usually requires dedicated organic synthesis labs. The large pore reticular MOFs also have the potential to partially lose porosity upon solvent removal.[7,26] Introducing stable hierarchical porosity by intergrowth is another method to broaden the pore size distribution.[27] There have been very few reports on extending MOF pore size distribution only by intergrowth. The existing works on MOF intergrowth mainly focus on limited systems exclusively on the micron-scale,[17-18,21] and the dissolution of seed particles remains a common issue.[28-29] In this work, we show a general procedure to synthesize intergrown hierarchical pillared MOF nanoparticles by controlling synthesis conditions only. 2,6-di-tert-butylpyridine (DTBP) was used as a (Brønsted) base to facilitate intergrowth at room temperature, where the weak Lewis basicity of DTBP resulting from steric hindrance would not lead to individual nucleation or modify the structure of MOF seed particles by coordination. In addition, we show that the mesoporosity created by hierarchical features from intergrowth MOF led to increased adsorption amount of methane, ethane, ethene, propane, and propene pure gases compared to pillared MOF seed particles at pressures ranging from 10^{-5}–10 bar (absolute). Results from adsorption have shown that the hierarchical MOFs not only adsorbed more gas comparing to the seed particles, they have also shown high selectivity in C_2/CH_4 and C_3/CH_4 adsorption (according to IAST calculations at total pressure 1 bar and CH_4 mole fraction 0.8).

The hierarchical MOFs were synthesized based on a typical seeded growth approach: seed particles with metal center M^{I} are placed in a seeded growth solution for M^{II} MOF to achieve intergrowth. The seed particles were chosen to be the pillared MOF

[a] *Department of Chemical Engineering, The Pennsylvania State University, University Park, PA 16802, USA, E-mail: xuz32@psu.edu.*

† Footnotes relating to the title and/or authors should appear here.

Electronic Supplementary Information (ESI) available: [details of any supplementary information available should be included here]. See DOI: 10.1039/x0xx00000x

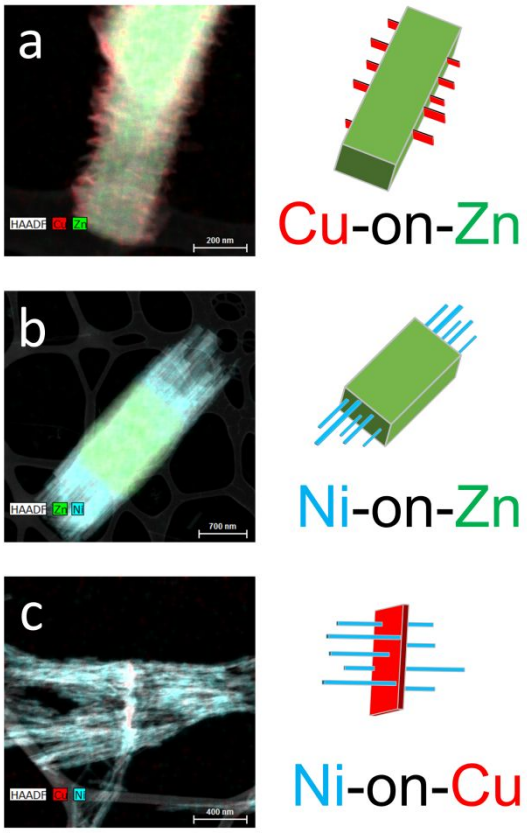

Figure 1. TEM micrograph of representative M^{II}-on-M^{I} MOF, (a) Cu-on-Zn; (b) Ni-on-Zn; (c) Ni-on-Cu

$M^{I}_2(ndc)_2(dabco)$ (M^{I}=Co, Ni, Cu, Zn), due to their highly tunable chemical structure, anisotropic crystalline structure, and robust synthesis conditions. The syntheses of the seed particles were achieved based on previously reported methods [30,31] (detailed procedure included in the experimental section). The different metal centers give the seed particles distinct morphologies: Cu MOF particles are plates, Zn MOF and Co MOF particles are rods, and Ni MOF particles are needles (Figure 1). Powder XRD has shown that all the seed particles have the pillared MOF structure,[30] variation in peak widths are from the small dimensions of some seed particles (Figure S1). Rietveld refinement of powder XRD patterns have shown (Figure S13-S15) that the structures of Zn, Ni and Co MOFs are isomorphous to $Cu_2(ndc)_2(dabco)$. [17]

The anisotropic intergrowth of MOF^{II}-on-MOF^{I} is attributed to the electronic structures of respective metals and their asymmetric coordination with linkers [32-34]. The anisotropic coordination leads to different growth rates along axial (z) and equatorial (x,y) directions. When coordinated with linkers, d^9 Cu(II) as paddle wheel center shows faster coordination on the equatorial plane (x,y) than along the axial (z) direction. Contrary to Cu(II), d^{10} Zn(II) and d^8 Ni(II) show faster axial coordination. Further, the slowest growing direction dominate the growth morphology of the crystal [35]. In agreement with the theory, the following relations have been experimentally observed from the morphologies of the seed particles: axial growth rate: Ni>Zn>Cu and equatorial growth rate: Cu>Zn>Ni. Specifically, Zn and Ni MOF^{I} grow faster along metal-dabco direction which result in rod shaped particles. However, Cu MOF^{I} grow faster along metal-ndc direction and result in 2D sheets.

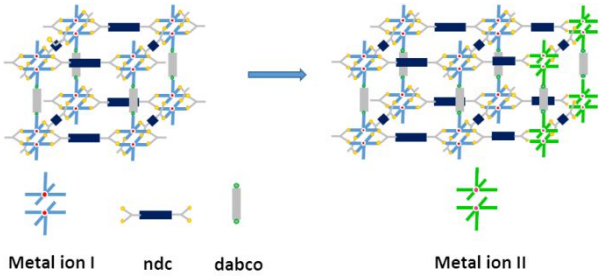

$Metal^{I}$ + Acid Linker + Base Linker + Additional base
$\leftrightarrow$ MOF^{I} (seed) + H^+ [R1]
$Metal^{II}$ + Acid Linker + Base Linker + Additional base + MOF^{I}
$\leftrightarrow$ MOF^{II}-on-MOF^{I} (intergrowth) + H^+ [R2]

Scheme 1. Reactions involved in the synthesis of M^{I} MOF seed particles (R1) and intergrowth of M^{II} MOF on M^{I} seeds. The reactions are hypothesized to be reversible.

The anisotropic growth theory also applies to secondary growth: the attachment rate of M^{II} (of MOF^{II}) on the surface of MOF^{I} determines the orientation of the secondary growth. For example, Cu MOF^{II}-on-Zn MOF^{I} secondary growth is initiated by the preferential bonding between Cu and ndc linkers at the equatorial directions of the Zn paddlewheel, which leads to growth of Cu MOF^{II} along the equatorial plane (Figure 1a). While Ni favored coordinate with dabco (axial direction) for Ni-on-Cu and Ni-on-Zn, which leads to dominating growth of Ni MOF^{II} along the axial direction (Figure 1b and 1c). As a result, MOF^{II} attached on MOF^{I} along their preferred directions and remain their individual morphologies. Seeded growth of heterometallic MOFs combines features of both seed and secondary particles, where their respective distinct morphologies were preserved. For example, Ni-on-Zn particles show needle-shaped Ni MOF perpendicularly grown onto rod-shape Zn MOF. The morphology of this particular intergrowth is also shown in Figure 2b and 2c. Electron diffraction patterns were taken on the seed particle and the secondary growth on Ni-on-Zn MOF as an example (Figure 2d and 2e), in order to investigate the crystalline orientation of these two parts. Diffraction spots with the same orientation from both the seed particle and the secondary growth show that secondary MOF particles are aligned and bound with seed particles, and that the two parts are not loosely attached.

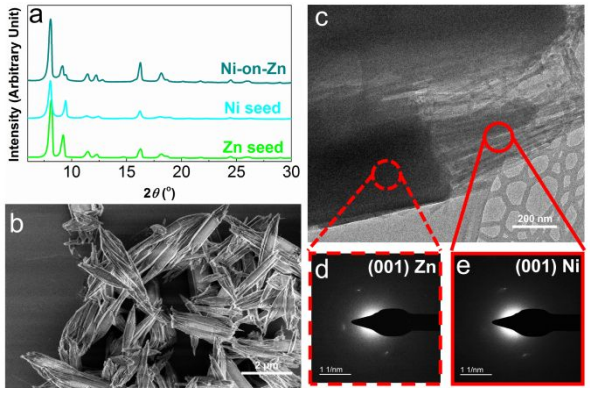

Figure 2. Structure and morphology of Ni-on-Zn intergrowth. (a) XRD patterns of Ni-on-Zn, Ni seed and Zn seed showing that the intergrowth is crystalline; (b) SEM image of Ni-on-Zn showing the intergrowth morphology; (c) TEM image of the intergrowth showing two distinct features in one particle. (d-e) TEM and electron diffraction from the seed and the secondary MOF within one Ni-on-Zn particle.

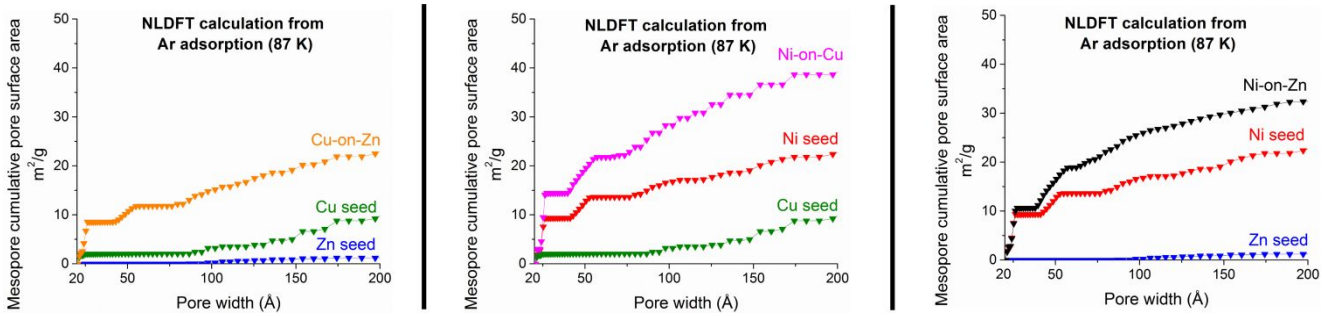

Figure 3. Cumulative pore surface area 2-20nm measured by Ar adsorption at 87K for: (a) Cu-on-Zn, Cu and Zn seed, (b) Ni-on-Cu, Ni and Cu seed, (c) Ni-on-Zn, Ni and Zn seed.

Interparticle spaces in Fig. 2(c) between the Ni MOF needles, indicating the presence of additional porosity formed by the seeded growth. This existence of the additional porosity is confirmed by consistently increasing cumulative pore area over a pore width of 2 nm – 20 nm calculated from Ar adsorption (Figure 3, S6).

Syntheses of all 12 permutations of heterometallic intergrowth involving Cu, Ni, Co, and Zn were achieved using this seeded growth method. The intergrowths are denoted as M^{II}-on-M^{I}, where M^{I} is the metal in the seed particle, and M^{II} is the metal in the MOF secondary growth. The representative micrographs of all 12 intergrowths are shown in Figure 1 (details shown in Figures S2). Different metals are shown in different colors to differentiate the primary (seed) particles and the secondary particles. Powder XRD patterns from all 12 intergrowths are shown in Figure S1. This proves that no additional phases were formed during the intergrowth. Presence of peaks from pillared MOF of both metal are due to minor mismatches of lattice parameters, that are shown not to prevent intergrowth from occurring.[17] In addition, the variations in peak widths are due to the presence of small dimensions, such as nanosheets and needles.

Scheme 1 shows the reactions for seed particle formation and secondary growth. We believe the successful secondary growth was due to careful control of reaction conditions.

Although it is well known that the presence of H^+ in MOF synthesis eventually can lead to dissolution of MOF, and that this situation can be remediated by adding base to the synthesis system[36], we believe in the case of seeded growth, a careful choice of base is critical to ensure the growth rate is faster than the dissolution rate. As a result, the morphology of MOF^{I} seed particles were preserved and MOF^{II} grew on MOF^{I}. In reaction R1, the presence of H^+ results from the deprotonation of acid linker and the incorporation of the anions into the MOF framework. Following seed synthesis step, residual H^+ can be brought to mix with secondary precursors by addition of the seed dispersion. As the reaction proceeds, accumulation of H^+ on the product side can lead to the dissolution of MOF^{I} and prevent MOF^{II}-on-MOF^{I} from formation. Removal of H^+ and other soluble products by washing with solvent after the synthesis is one option to reduce the H^+ level at the end of the synthesis. However, we believe that controlling the level of H^+ during synthesis is the best option. Amines and its derivatives have been utilized by others to prevent dissolution of MOF back to precursors during secondary growth, for instance, N-ethyldiisopropylamine (EDIPA) prevents IRMOF-1 from degradation.[29] Contrary to EDIPA mentioned above, 2,6-di-tert-butylpyridine (DTBP) captures H^+ effectively but will not act as a strong Lewis base, because its Lewis basicity is sterically hindrance by the tert-butyl groups. Therefore, DTBP was used in all systems to prevent dissolution of MOF particles, and was shown to be applicable to all 12 intergrowths.

Polar aprotic solvents were chosen for seed and secondary synthesis of MOF particles. A solvent for MOF synthesis should have relatively good solubility of metal ions and linkers. Polar solvent is chosen due to its large dipole moment enabling it to dissolve precursors. Different solvent has different ability to distinguish the acidity of different acid linkers.[37] Aprotic solvent can keep the concentration of H^+ at relatively low levels comparing to highly protic solvents such as methanol. Acetone is selected as solvent since they are polar aprotic solvent with relatively good solubility for linkers. Therefore, seeded growth is facilitated by controlling H^+ and preventing seeds from dissolution with a polar aprotic solvent.

The concept of hierarchical MOFs in this study was conceived based on the expectation that the hierarchical features created from the additional porosity will increase adsorption amounts of hydrocarbons. Three hierarchical intergrowths were chosen for the study of hydrocarbon adsorption (Figure.3,4). The adsorption of methane, ethane, ethene, propane, and propene were tested on the hierarchical MOFs. The isotherms of hydrocarbon adsorption on the intergrowth MOF are shown in Figure S3, S4 and S5, as a representative set of isotherms of intergrown MOFs. Firstly, there are no differences in the adsorption amount of alkane and alkene of the same carbon number, indicating that the increased adsorption amount is not due to chemical adsorption on unsaturated metal sites (such as the case of alkene adsorption on MOF-74). The adsorption amounts of hydrocarbons on the heterometallic intergrowth MOFs M^{II}-on-M^{I} are greatly increased compared to the primary microporous M^{I} MOF especially Zn MOF. In order to understand the origin of the increased gas adsorption amount, the mesopore volume and area of these materials were studied by Ar adsorption. We observe that there are higher cumulative mesopore volume and mesopore area created by the

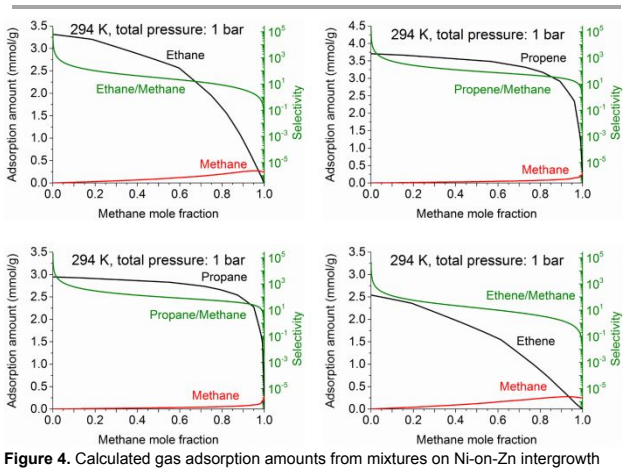

Figure 4. Calculated gas adsorption amounts from mixtures on Ni-on-Zn intergrowth based on IAST (ideal adsorbed solution theory): (a) ethane/methane mixture, (b) ethene/methane mixture, (c) propane/methane mixture, (d) propene/methane mixture. Calculations were performed for 294 K and a total pressure of 1 bar (absolute).

intergrowth (Figure 3, S6). We believe polarizability effect dominant in adsorption process which indicates MOF with larger polar surface area is a good adsorbent candidate.[38] The naphthalene ring from ndc and N atom from dabco provide a polar environment through conjugated π electron reservoir.[39] The following polarizability trend: propane, propene > ethane, ethane > methane[1] explains the favorable adsorption of C_3 and results in selective adsorption. Also, the intergrown MOF created easily accessible mesopore surface that exhibits polarity. The higher polar surface area and volume compare to seed MOF explains improved adsorption capacity. The above led us to believe that the additional mesopores created by the hierarchical features are responsible for the increased amount adsorbed of all molecules, especially the C_2 and C_3 hydrocarbons investigated in this study.

Inspired by the different amount of gases adsorbed at low pressures, as well as the steep isotherms of C_2 and C_3 hydrocarbons, we expect that the materials could be used for removing C_2 and C_3 hydrocarbons (natural gas liquids) from natural gas by adsorption (such as pressure-swing adsorption or vacuum-swing adsorption). We calculated mixed gas adsorption selectivity using the IAST (ideal adsorbed solution theory) from single gas adsorption data.[40] Predicted C_3/methane adsorption selectivity was shown to be approximately 50 with a 101.3 kPa total pressure and 20% C_3 and 80% methane gas phase. Additional predicted selectivities are shown in Supporting Information (Figures S7-S11, Table S1).

Conclusions

In conclusion, we have demonstrated that the heterometallic intergrowth of two pillared MOFs can be achieved among Cu, Zn, Ni and Co. A general strategy involving controlling the Brønsted acid, Lewis base, and solvents for synthesis was the key to successful intergrowths of the MOFs. The intergrowths show hierarchical morphology and porosity. The 2-20 nm mesopores were responsible for adsorbing increased amounts of light hydrocarbons. The materials also showed high adsorptive selectivity for light hydrocarbon/CH_4 separation.

Conflicts of interest

There are no conflicts to declare.

Acknowledgements

The authors acknowledge the financial support from the 3M Company (3M Non-Tenured Faculty Award), the Department of Chemical Engineering at the Pennsylvania State University, and the Institute for Natural Gas Research (INGaR) at the Pennsylvania State University. X.Z. acknowledges financial support from the John J. and Jean M. Brennan Clean Energy Early Career Professorship. Materials characterization was performed at the Materials Characterization Laboratory, which is a partner in the National Nanotechnology Infrastructure Network (NNIN) and the Materials Research Facilities Network (MRFN), supported by the U.S. National Science Foundation (award DMR-1420620).

References

1 J.-R. Li, R. J. Kuppler, H.-C. Zhou, "Selective gas adsorption and separation in metal–organic frameworks." *Chemical Society Reviews* **2009**, *38*, 1477-1504.
2 J. Gascon, F. Kapteijn, "Metal-Organic Framework Membranes—High Potential, Bright Future?." *Angewandte Chemie International Edition* **2010**, *49*, 1530-1532.
3 J. Caro, "Are MOF membranes better in gas separation than those made of zeolites?." *Current Opinion in Chemical Engineering* **2011**, *1*, 77-83.
4 J. Li, S. Cheng, Q. Zhao, P. Long, J. Dong, "Synthesis and hydrogen-storage behavior of metal–organic framework MOF-5." *international journal of hydrogen energy* **2009**, *34*, 1377-1382.
5 L. C. Lin, J. Kim, X. Kong, E. Scott, T. M. McDonald, J. R. Long, J. A. Reimer, B. Smit, "Understanding CO2 dynamics in metal–organic frameworks with open metal sites." *Angewandte Chemie International Edition* **2013**, *52*, 4410-4413.
6 H. Bux, C. Chmelik, R. Krishna, J. Caro, "Ethene/ethane separation by the MOF membrane ZIF-8: molecular correlation of permeation, adsorption, diffusion." *Journal of membrane science* **2011**, *369*, 284-289.
7 D. Yuan, D. Zhao, D. Sun, H. C. Zhou, "An isoreticular series of metal–organic frameworks with dendritic hexacarboxylate ligands and exceptionally high gas-uptake capacity." *Angewandte Chemie International Edition* 2010, 49, 5357-5361.
8 H. T. Kwon, H.-K. Jeong, A. S. Lee, H. S. An, J. S. Lee, "Heteroepitaxially grown zeolitic imidazolate framework membranes with unprecedented propylene/propane separation performances." *Journal of the American Chemical Society* 2015, 137, 12304-12311.
9 H. Li, M. Eddaoudi, M. O'Keeffe, O. M. Yaghi, "Design and synthesis of an exceptionally stable and highly porous metal-organic framework." *nature* **1999**, *402*, 276.
10 D. Britt, D. Tranchemontagne, O. M. Yaghi, "Metal-organic frameworks with high capacity and selectivity for harmful gases." *Proceedings of the National Academy of Sciences* **2008**, *105*, 11623-11627.
11 J. Lee, O. K. Farha, J. Roberts, K. A. Scheidt, S. T. Nguyen, J. T. Hupp, "Metal–organic framework materials as catalysts." *Chemical Society Reviews* **2009**, *38*, 1450-1459.
12 L. E. Kreno, K. Leong, O. K. Farha, M. Allendorf, R. P. Van Duyne, J. T. Hupp, "Metal–organic framework materials as chemical sensors." *Chemical reviews* **2011**, *112*, 1105-1125.
13 L. Yang, N. Yi, J. Zhu, Z. Cheng, X. Yin, X. Zhang, H. Zhu, H. Cheng, "Novel gas sensing platform based on a stretchable laser-induced graphene pattern with self-heating capabilities." *Journal of Materials Chemistry A* **2020**.
14 H. Deng, C. J. Doonan, H. Furukawa, R. B. Ferreira, J. Towne, C. B. Knobler, B. Wang, O. M. Yaghi, "Multiple functional groups of varying ratios in metal-organic frameworks." *Science* **2010**, *327*, 846-850.
15 Z. Wang, S. M. Cohen, "Postsynthetic covalent modification of a neutral metal– organic framework." *Journal of the American Chemical Society* **2007**, *129*, 12368-12369.
16 M. Kim, J. F. Cahill, H. Fei, K. A. Prather, S. M. Cohen, "Postsynthetic ligand and cation exchange in robust metal–organic frameworks." *Journal of the American Chemical Society* **2012**, *134*, 18082-18088.
17 S. Furukawa, K. Hirai, K. Nakagawa, Y. Takashima, R. Matsuda, T. Tsuruoka, M. Kondo, R. Haruki, D. Tanaka, H. Sakamoto,

"Heterogeneously hybridized porous coordination polymer crystals: fabrication of heterometallic core–shell single crystals with an in-plane rotational epitaxial relationship." *Angewandte Chemie International Edition* **2009**, *48*, 1766-1770.
18 K. Koh, A. G. Wong-Foy, A. J. Matzger, "MOF@ MOF: microporous core–shell architectures." *Chemical Communications* **2009**, 6162-6164.
19 H. J. Lee, Y. J. Cho, W. Cho, M. Oh, "Controlled isotropic or anisotropic nanoscale growth of coordination polymers: formation of hybrid coordination polymer particles." *Acs Nano* **2012**, *7*, 491-499.
20 S. Choi, T. Kim, H. Ji, H. J. Lee, M. Oh, "Isotropic and Anisotropic Growth of Metal–Organic Framework (MOF) on MOF: Logical Inference on MOF Structure Based on Growth Behavior and Morphological Feature." *Journal of the American Chemical Society* **2016**, *138*, 14434-14440.
21 S. Furukawa, K. Hirai, Y. Takashima, K. Nakagawa, M. Kondo, T. Tsuruoka, O. Sakata, S. Kitagawa, "A block PCP crystal: anisotropic hybridization of porous coordination polymers by face-selective epitaxial growth." *Chemical Communications* **2009**, 5097-5099.
22 N. Zhou, F. Su, C. Guo, L. He, Z. Jia, M. Wang, Q. Jia, Z. Zhang, S. Lu, "Two-dimensional oriented growth of Zn-MOF-on-Zr-MOF architecture: A highly sensitive and selective platform for detecting cancer markers." *Biosensors and Bioelectronics* **2019**, *123*, 51-58.
23 M. Eddaoudi, J. Kim, N. Rosi, D. Vodak, J. Wachter, M. O'keeffe, O. M. Yaghi, "Systematic design of pore size and functionality in isoreticular MOFs and their application in methane storage." *Science* **2002**, *295*, 469-472.
24 R. Banerjee, H. Furukawa, D. Britt, C. Knobler, M. O'Keeffe, O. M. Yaghi, "Control of pore size and functionality in isoreticular zeolitic imidazolate frameworks and their carbon dioxide selective capture properties." *Journal of the American Chemical Society* **2009**, *131*, 3875-3877.
25 H. Deng, S. Grunder, K. E. Cordova, C. Valente, H. Furukawa, M. Hmadeh, F. Gándara, A. C. Whalley, Z. Liu, S. Asahina, "Large-pore apertures in a series of metal-organic frameworks." *science* **2012**, *336*, 1018-1023.
26 O. M. Yaghi, H. Li, C. Davis, D. Richardson, T. L. Groy, "Synthetic strategies, structure patterns, and emerging properties in the chemistry of modular porous solids." *Accounts of Chemical Research* **1998**, *31*, 474-484.
27 W. Chaikittisilp, Y. Suzuki, R. R. Mukti, T. Suzuki, K. Sugita, K. Itabashi, A. Shimojima, T. Okubo, "Formation of hierarchically organized zeolites by sequential intergrowth." *Angewandte Chemie International Edition* **2013**, *52*, 3355-3359.
28 Z. Zhang, Y. Chen, S. He, J. Zhang, X. Xu, Y. Yang, F. Nosheen, F. Saleem, W. He, X. Wang, "Hierarchical Zn/Ni-MOF-2 nanosheet-assembled hollow nanocubes for multicomponent catalytic reactions." *Angewandte Chemie International Edition* **2014**, *53*, 12517-12521.
29 Y. Yoo, H.-K. Jeong, "Heteroepitaxial Growth of Isoreticular Metal− Organic Frameworks and Their Hybrid Films." *Crystal Growth & Design* **2010**, *10*, 1283-1288.
30 S. Mahdian, M. R. Naimi - Jamal, L. Panahi, "Activity of M2 (BDC) 2 (DABCO)(M= Co, Ni, Cu and Zn) Metal-Organic Frameworks Prepared via Ball-Milling Solvent-Free Method in Acylation of Alcohols, Amines and Aldehydes." *ChemistrySelect* **2018**, *3*, 11223-11229.
31 J. Zha, X. Zhang, "Room-temperature synthesis of two-dimensional metal–organic frameworks with controllable size and functionality for enhanced CO2 sorption." *Crystal Growth & Design* **2018**, *18*, 3209-3214.
32 R. Deeth, M. Gerloch, "Ligand-field parameters and the stereochemical activity of d shells in trigonal-bipyramidal complexes of the first transition series." *Inorganic Chemistry* **1985**, *24*, 4490-4493.
33 K. Alzahrani, R. Deeth, "Density functional calculations reveal a flexible version of the copper paddlewheel unit: implications for metal organic frameworks." *Dalton Transactions* **2016**, *45*, 11944-11948.
34 T. Tsuruoka, S. Furukawa, Y. Takashima, K. Yoshida, S. Isoda, S. Kitagawa, "Nanoporous nanorods fabricated by coordination modulation and oriented attachment growth." *Angewandte Chemie* **2009**, *121*, 4833-4837.
35 A. Umemura, S. Diring, S. Furukawa, H. Uehara, T. Tsuruoka, S. Kitagawa, "Morphology design of porous coordination polymer crystals by coordination modulation." *Journal of the American Chemical Society* **2011**, *133*, 15506-15513.
36 Y. Yoo, Z. Lai, H.-K. Jeong, "Fabrication of MOF-5 membranes using microwave-induced rapid seeding and solvothermal secondary growth." *Microporous and mesoporous materials* **2009**, *123*, 100-106.
37 K. Sarmini, E. Kenndler, "Ionization constants of weak acids and bases in organic solvents." *Journal of biochemical and biophysical methods* **1999**, *38*, 123-137.
38 R. T. Yang, *Adsorbents: fundamentals and applications*, John Wiley & Sons, **2003**.
39 Y. Zou, S. Hong, M. Park, H. Chun, M. S. Lah, "Selective gas sorption property of an interdigitated 3-D metal–organic framework with 1-D channels." *Chemical communications* **2007**, 5182-5184.
40 A. L. Myers, J. M. Prausnitz, Thermodynamics of mixed-gas adsorption." *AIChE journal* **1965**, *11*, 121-127.